

# Which Density Functional Is the Best in Computing C–H Activation Energies by Pincer Complexes of Late Platinum Group Metals?

Wenzhen Lai,<sup>\*,†</sup> Jiannian Yao,<sup>‡</sup> Sason Shaik,<sup>§</sup> and Hui Chen<sup>\*,‡</sup>

<sup>†</sup>Department of Chemistry, Renmin University of China, Beijing, 100872, China

<sup>‡</sup>Beijing National Laboratory for Molecular Sciences (BNLMS), CAS Key Laboratory of Photochemistry, Institute of Chemistry, Chinese Academy of Sciences, Beijing, 100190, China

<sup>§</sup>Institute of Chemistry and the Lise Meitner-Minerva Center for Computational Quantum Chemistry, Hebrew University of Jerusalem, Givat Ram Campus, 91904 Jerusalem, Israel

## S Supporting Information

**ABSTRACT:** Using the recently proposed corrective LCCSD(T) method as a reference, we systematically assess the widely used approximate density functionals to reproduce C–H bond activation barriers by pincer complexes of the late platinum group transition metals (TMs) (TM = Rh, Pd, Ir, Pt). The pincer ligands explored here cover a wide range of PNP, PCP, POCOP, NCN, and SCS types. Interestingly, B3LYP is found to be the most accurate functional, followed by several others previously identified as well-performing functionals, like B2GP-PLYP, B2-PLYP, and PBE0. However, all tested functionals were found to exhibit the following uniform trends: (1) the DFT barriers for reactions of group 9 TM (Rh and Ir) pincer complexes show higher accuracy compared with those for group 10 TM (Pd and Pt) reactions; (2) within the same group, 5d TM pincer complexes have higher accuracy than 4d TM ones. Consequently, the barriers for C–H activation by Pd(II) pincer complexes were found to be the least accurate among the four TMs in almost all functionals tested here. The DFT empirical dispersion correction (DFT-D3) is shown to have a very small effect on barrier height. This study has some implications for other  $\sigma$ -bond activations like H–H, C–C, and C–halogen bonds by late platinum group pincer complexes.

Pincer ligands are tridentate ligands that favor meridional coordination in one plane. Pincer complexes have evolved to be one of the most versatile classes in organometallic chemistry, with many applications in areas of homogeneous catalysis, enantioselective organic transformations, activation of strong bonds, etc.<sup>1–4</sup> This success was followed by many density functional theory (DFT) studies which explored the reaction mechanisms of pincer complexes of late platinum group transition metals (TMs).<sup>5</sup> These theoretical studies covered all late platinum group TMs; Ir,<sup>5a–r</sup> Rh,<sup>5m–t</sup> Pt,<sup>5m–o,u,v</sup> and Pd.<sup>5n,o,w–z</sup> In many reactions by late platinum group TM pincer complexes,<sup>5</sup> C–H activation, which is characterized by C–H bond cleavage, is inevitably involved. Being a chemical issue of major interest, the C–H activation process is among the most extensively explored research areas. Discovering and understanding the reaction mechanism and reactivity patterns in this reaction is therefore essential and may be helpful in designing new catalysts for C–H activation process. Though DFT methods have achieved great success in exploring the TM-catalyzed reaction mechanisms,<sup>6</sup> the quantitative aspect of barrier height computations in DFT is still shrouded in doubt. As such, high level ab initio methods such as coupled cluster can serve as benchmark tools for the calibration and selection of the best DFT methods.<sup>7–17</sup> Unfortunately, the use of traditional canonical coupled cluster (CC) methods like CCSD(T), the “gold standard” in modern quantum chemistry calculations for closed-shell systems, is limited by high computational cost and steep scaling with system size. New methods must be sought.

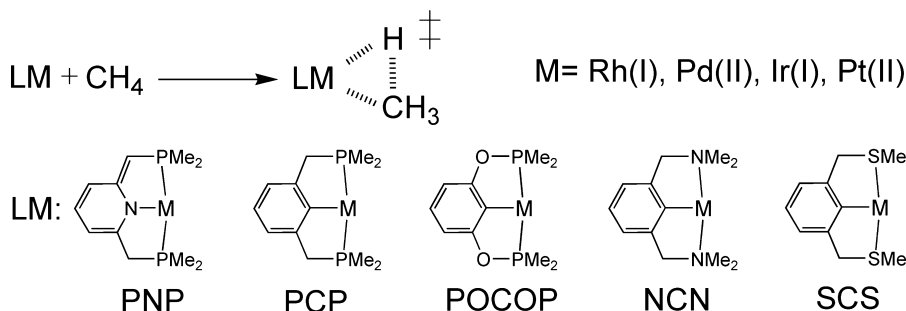
Recently, we developed a corrective scheme for improving the accuracy of local coupled cluster (LCC) methods, which can be applied to larger and hence more realistic systems.<sup>18</sup> Test computations of various catalytic reactions by 5d-TM (Ir, Pt, Au) complexes indicated that this corrective LCC method is very accurate, on par with the CCSD(T)/CBS reference results, with a mean unsigned deviation (MUD) of about 0.3 kcal/mol and maximum deviation (MaxD) of about 0.9 kcal/mol. Especially promising is that the deviation of only 0.09 kcal/mol from CCSD(T)/CBS was found for C–H activation catalyzed by the Ir(I) PNP pincer complex included in our test set, which is obviously enough for DFT calibration purpose. In addition, the maximum deviation of C–H activation barriers for all four tested different types of Ir and Pt catalysts was only 0.13 kcal/mol,<sup>19</sup> which demonstrates the robustness and effectiveness of our corrective LCC method in C–H activation barrier computation. In this work, we propose the new corrective LCC method<sup>18</sup> as a yardstick for assessing the performance of various DFT methods on methane C–H activation barriers for various late platinum group TM (Rh, Pd, Ir, Pt) pincer complexes, which are depicted in Scheme 1. The pincer ligands tested herein included a wide range of PNP, PCP, POCOP, NCN, and SCS types. All of these pincer complexes correspond to experimental systems.

The so assessed functionals, in this work, include the widely used PBE,<sup>19a</sup> PBE0,<sup>19</sup> M06,<sup>20</sup> M06-L,<sup>20a</sup> M06-2X,<sup>20</sup> TPSS,<sup>21</sup> TPSSH,<sup>21</sup> B3LYP,<sup>22</sup> B2GP-PLYP,<sup>23</sup> B2-PLYP,<sup>24</sup> wB97X,<sup>25</sup> and

Received: July 12, 2012

Published: August 22, 2012

Scheme 1. Pincer Complexes for Methane C–H Activation Studied in This Work



BMK<sup>26</sup> methods. As such, these functionals cover a wide spectrum of GGA, meta-GGA, hybrid, double hybrid, and range-separated functionals. Except for general-purpose functionals, we tested also two “kinetic” functionals (M06-2X and BMK), optimized for barrier heights of main-group reactions and containing a high percentage of Hartree–Fock (HF) exchange.

The pincer TM-CH<sub>4</sub>  $\sigma$  reactant complex (RC) and C–H activation transition state (TS) were fully optimized with the TPSS functional, using Ahlrich’s triple- $\zeta$  polarized def-TZVP basis set.<sup>27</sup> Geometry optimization of TSs was tested also for some pincer complexes by using other functionals including M06L, PBE0, B2-PLYP, BP86, and B3LYP. The results in Table S1 of the Supporting Information (SI) document indicate that with few exceptions, all tested functionals produced similar TS structures. Vibrational analysis was performed to ensure that RC and TS are stationary points with no and one imaginary frequency, respectively. The DFT single-point calculations based on the optimized geometries were performed with the triple- $\zeta$  multiple polarized cc-pVTZ basis set.<sup>28</sup> In single point but not in geometry optimization calculations, the core electrons of non-hydrogen atoms were correlated in an MP2-type correlation treatment of double-hybrid functionals. It should be noted that the scalar relativistic effect for TMs is treated with different relativistic pseudopotentials (PP) in def-TZVP and cc-pVXZ series of basis sets. In def-TZVP, Stuttgart’s older MWB-type PPs are employed,<sup>29</sup> while in cc-pVXZ, new MCDHF PPs, which are meant to supersede the MWB PPs, are employed.<sup>28a,b</sup> All DFT calculations were done with the Gaussian 09 program package.<sup>30</sup>

The details of our corrective LCC method have been described in previous work<sup>18</sup> and will not be repeated here. The energetic correction ( $\Delta E(\text{LCC-LCC})$ ) for the LCC/DZ result used eq 1 (DZ represents double- $\zeta$  basis set such as cc-pVDZ), which is the most accurate corrective formula found previously.<sup>18</sup>

$$\Delta E(\text{LCC} - \text{LCC}) = (E_{\text{CC/DZ}} - E_{\text{LCC/DZ}}) + \Delta E_{\text{CBS-LCC}} \quad (1)$$

All ab initio single-point calculations employing CCSD(T) and LCCSD(T0) were carried out with the MOLPRO program package.<sup>31</sup> The basis sets used for C, H, O, N/S, P/TM are cc-pVXZ/cc-pV(X+D)Z/cc-pVXZ-PP (X = D,T),<sup>28</sup> which are denoted hereafter as XZ. To reduce the computational cost, all LCC calculations involve the density fitting approximations since it has a negligible effect on accuracy. To minimize fitting errors, we employed the corresponding auxiliary basis sets.<sup>32</sup>

The two-point extrapolations to the complete-basis set limit (CBS) were carried out for Hartree–Fock (HF) and

correlation energies separately. For the HF energy, we used the formula proposed by Martin and Karton<sup>33</sup> in eq 2. For the correlation energy, we used eq 3 proposed by Truhlar.<sup>34</sup>

$$E_{\text{HF},n} = E_{\text{HF,CBS}} + A \exp(-\alpha\sqrt{n}) \quad (2)$$

$$E_{\text{corr},n} = E_{\text{corr,CBS}} + \frac{A}{n^\beta} \quad (3)$$

DZ and TZ basis sets were employed in two-point CBS extrapolations. The predetermined optimal parameters  $\alpha$  and  $\beta$  are available for DZ-TZ extrapolation ( $\alpha = 4.42$ ,  $\beta = 2.46$ ).<sup>35</sup>

The standard orbital domains are generated from the procedure of Boughton and Pulay<sup>36</sup> using the default thresholds in MOLPRO. To improve the domain consistency, we manually merged the standard domains generated automatically from DZ and TZ basis sets, and from RC and TS. The default distance criteria ( $R_{\text{CLOSE}} = 1$  and  $R_{\text{WEAK}} = 3$  bohr) that control the pair classification were used. Using this default distance criteria generates only a difference of 0.06 kcal/mol compared with the almost converged distance criteria ( $R_{\text{CLOSE}} = 7$  and  $R_{\text{WEAK}} = 8$  bohr) for our corrected LCCSD(T0) activation energy of the PNP-Ir system (for details, see Table S2 in the SI). The outer core–valence correlation effect was tested previously for several Ir- and Pt-catalyzed C–H activation reactions, including the PNP-Ir pincer complex, and found to be small.<sup>37</sup> Thus, we did not consider the outer core–valence correlation effect here. Below we focus on the key results, and the full set of computational data is relegated to the SI.

The calculated corrected LCCSD(T0) activation energies for methane C–H activation by pincer complexes depicted in Scheme 1 are collected in Table 1. It is apparent that the C–H

**Table 1. Methane C–H Activation Energies  $\Delta E^\ddagger$  (kcal/mol) Calculated by the Corrective LCCSD(T0) Method for All Pincer Complexes Shown in Scheme 1**

$\Delta E^\ddagger$	PNP	PCP	POCOP	NCN	SCS
Rh(I)	10.95	21.60	19.66	22.29	22.60
Pd(II)	38.93	53.27	53.73	63.35	58.29
Ir(I)	1.54	11.12	9.49	12.79	13.63
Pt(II)	11.48	36.06	36.46	40.25	40.64

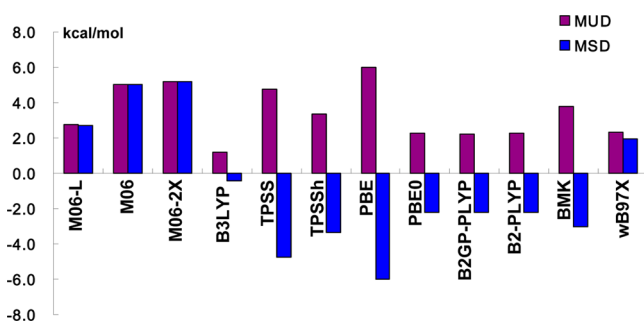
activation by all studied Pd pincer complexes has too high barriers to enable them to function as catalysts. On the contrary, Ir pincer complexes have quite low barriers (<14 kcal/mol) and can act as good catalysts for C–H activation, while Rh pincer complexes have higher barriers compared with the corresponding Ir pincer complexes, but still being considerably smaller than those of the corresponding Pd ones. These results

**Table 2.** MUD and MaxD (Inside Brackets) of the C–H Activation Energies (kcal/mol) Calculated at the Various DFT/TZ Levels for All Pincer Complexes Shown in Scheme 1 Taking the Corrected LCCSD(T0) Results as a Reference<sup>a</sup>

	M06-L	M06	M06-2X	B3LYP	TPSS	TPSSH	PBE	PBE0	B2GP-PLYP	B2-PLYP	BMK	wB97X <sup>h</sup>
HF% <sup>b</sup>	0	27	54	20	0	10	0	25	65	53	42	15
[Rh] <sup>c</sup>	2.16 (2.14) [2.96]	3.64 (3.57) [5.08]	4.23 (4.22) [5.67]	<b>0.76</b> (1.24) [−1.83]	4.28 (4.75) [−5.42]	3.17 (3.64) [−4.34]	5.01 (5.34) [−6.18]	2.05 (2.40) [−3.29]	2.52 (2.74) [−3.96]	2.36 (2.67) [−3.67]	3.96 (4.52) [−7.40]	0.99 (1.00) [2.22]
[Pd] <sup>d</sup>	2.27 (2.25) [5.19]	7.40 (7.34) [8.71]	10.86 (10.87) [12.69]	<b>1.96</b> (2.57) [−4.07]	8.23 (8.98) [−11.58]	5.37 (6.10) [−8.31]	9.84 (10.34) [−13.32]	2.64 (2.99) [−4.79]	3.34 (3.69) [−4.98]	3.79 (4.27) [−5.92]	4.99 (5.68) [−6.84]	5.49 (5.58) [7.36]
[Ir] <sup>e</sup>	3.23 (3.22) [3.92]	2.51 (2.46) [3.44]	2.16 (2.15) [3.72]	<b>0.72</b> (0.77) [1.25]	1.93 (2.39) [−3.61]	1.51 (2.00) [−3.20]	3.01 (3.34) [−4.55]	1.76 (2.13) [−3.35]	1.04 (1.29) [−2.23]	0.86 (1.14) [−1.96]	1.58 (2.09) [−2.83]	1.03 (1.02) [−2.04]
[Pt] <sup>f</sup>	3.38 (3.38) [4.44]	6.60 (6.53) [8.82]	3.56 (3.56) [6.21]	<b>1.23</b> (1.54) [−2.32]	4.65 (5.37) [−6.88]	3.35 (4.06) [−5.27]	6.20 (6.70) [−8.57]	2.63 (3.15) [−4.17]	1.91 (2.25) [−2.64]	2.03 (2.50) [−3.17]	4.60 (5.58) [−6.13]	1.75 (1.81) [2.65]
total <sup>g</sup>	2.76 (2.75)	5.04 (4.97)	5.20 (5.20)	<b>1.17</b> (1.53)	4.77 (5.37)	3.35 (3.95)	6.02 (6.43)	2.27 (2.67)	2.20 (2.49)	2.26 (2.65)	3.78 (4.46)	2.32 (2.35)

<sup>a</sup>MUD values with DFT-D3(0) are inside parentheses, and small MUD values are in bold. <sup>b</sup>Percentage of HF exchange in various functionals. <sup>c</sup>Deviations of five Rh pincer complexes. <sup>d</sup>Deviations of five Pd pincer complexes. <sup>e</sup>Deviations of five Ir pincer complexes. <sup>f</sup>Deviations of five Pt pincer complexes. <sup>g</sup>Deviations of all pincer complexes. <sup>h</sup>There are no DFT-D3(0) parameters for the wB97X functional; thus wB97XD (empirical dispersion corrected wB97X defined in ref 39 from the developers of this functional) was used instead.

about C–H activation reactivity are largely in line with the known trends for these late platinum group pincer complexes.<sup>1–5</sup> In addition, for Pt, only PNP-Pt encounters a small barrier of 11.48 kcal/mol; other Pt complexes have very high barriers. For all four metals, the barrier variations due to ligand variation are apparent, indicating that pincer ligands play an important role in determining the C–H activation barrier. Using these data as a reference, our calibration results for the various DFT methods on C–H activation energies of pincer complexes are summarized in Table 2 and depicted in Figure 1.

**Figure 1.** Mean unsigned (MUD) and signed (MSD) deviations of calculated activation energies of all reactions in Scheme 1, calculated with various DFT/TZ methods without dispersion correction D3(0) taking corrected LCC values as a reference.

Interestingly, almost all DFTs (with some exceptions of M06-L and wB97X) tested in this work demonstrate some uniform trends. First, for either group 9 or group 10 TMs, the 4d TM containing pincer complexes exhibit larger errors in DFT barrier height calculations compared with the corresponding 5d TMs. Second, in either 4d or 5d TMs, group 9 TM complexes exhibit smaller errors in DFT barrier height calculations than the corresponding group 10 ones. As a result, for almost all functionals tested herein (with a notable exception of M06-L),<sup>38</sup> Pd pincer complexes are most difficult to treat accurately among the four late platinum group TMs tested herein. Previous extensive DFT calibration studies for reaction barriers

were done mostly to neutral Pd(0) rather than to the Pd(II) species studied herein.<sup>7–10</sup> These trends, hitherto unknown for pincer complexes, are intriguing and deserving of future exploration in other types of ligands and reactions. It would be particularly interesting to know if other platinum group TMs, i.e. Ru and Os, follow these trends too.

From Figure 1 and Table 2, it can be seen that the smallest deviations are calculated from the B3LYP functional, which gives 1.17 kcal/mol MUD and −4.07 kcal/mol MaxD and is the only one having a MUD of less than 2 kcal/mol among all tested functionals. This result is unusual and somewhat surprising since recent DFT calibration studies<sup>40,41</sup> for TM-containing systems other than pincer complexes seldom identified B3LYP to be the best functional,<sup>42</sup> even though it is still the most popular functional in computational chemistry.<sup>43</sup> This finding clearly shows the necessity to perform DFT calibrations reliably before voicing an opinion for any specific case.

It can be seen from Table 1 and Figure 1 that, except for B3LYP, there are several functionals with MUDs between 2 and 3 kcal/mol. These functionals are (in the order of increasing MUD) B2GP-PLYP < B2-PLYP < PBE0 < wB97X < M06-L. The largest absolute values of MaxD for these five functionals are between about 5 and 7 kcal/mol, with wB97X having the largest MaxD. It should be noted that if balanced performance of all pincer systems is required, then wB97X is the less suitable among these relatively well performing functionals because it has comparatively large errors for Pd systems than for the other three TM pincer complexes. The three well performing functionals B2GP-PLYP, B2-PLYP, and PBE0 conform with our previous similar findings for Ir-/Pt-/Au-catalyzed reactions and Au-substrate binding.<sup>18,44</sup>

As found before in other TM-containing systems,<sup>10,18</sup> the “kinetic” functionals M06-2X and BMK, which contain a high percentage of HF exchange, as needed for good performance in main-group reactions barriers, do not perform well in C–H activation reaction barriers of late-TM pincer complexes, especially for Pd systems. Thus, a high percentage of HF exchange by itself is not beneficial in this regard, and double

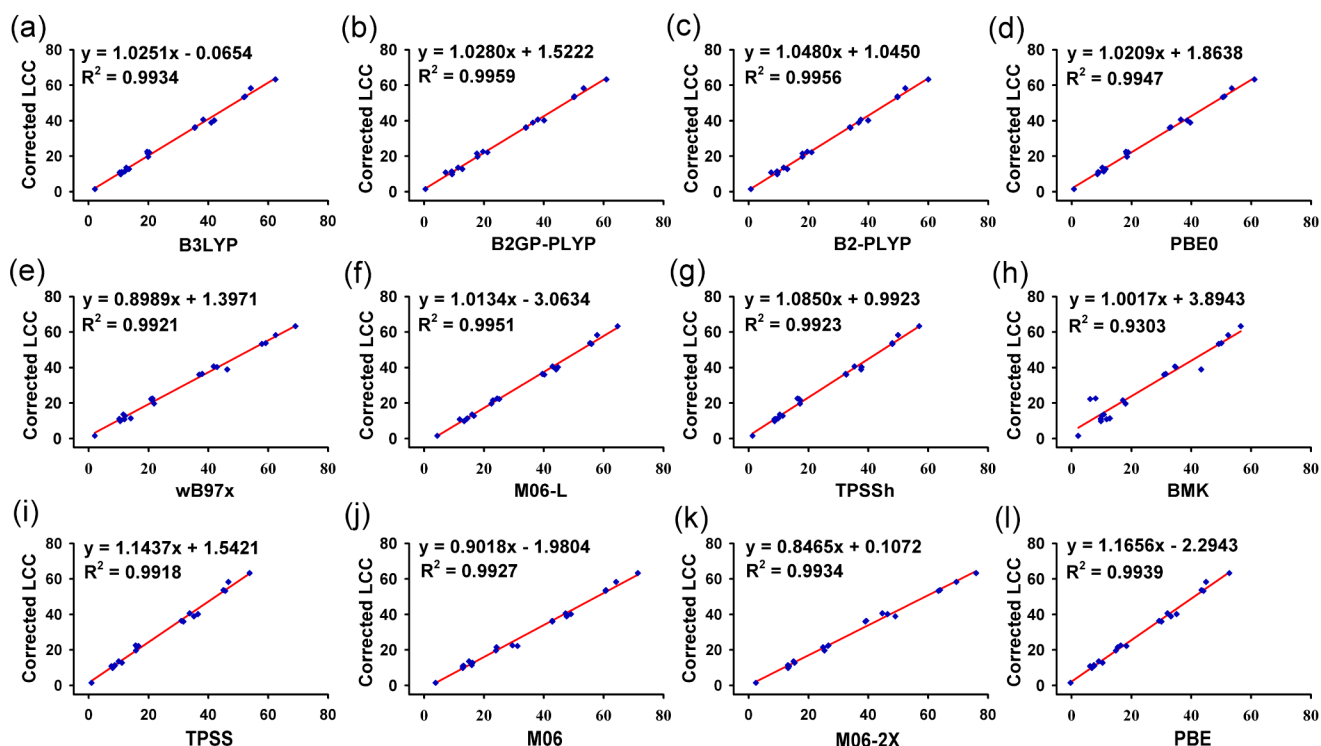


Figure 2. The correlations of all calculated barriers (kcal/mol) in this study between corrected LCC values and various DFT values.

hybrid functionals with both a high percentage of nonlocal HF exchange and a nonlocal correlation contribution (MP2-type) like in B2GP-PLYP and B2-PLYP appear to be able to alleviate this deficiency.

The above consideration ranks the DFT performance in terms of absolute barrier heights. Often more important in reaction mechanism studies is the trend discovery. To explore this aspect of DFT performance, we plotted the 20 DFT-computed barriers with the corresponding corrected LCC values as shown in Figure 2. It can be seen that despite the differences in absolute barrier performance, all functionals possess excellent correlations with  $R^2$  very close to 1.0, with the exception of BMK for which  $R^2 = 0.93$ . This means that for the pincer systems under study, DFT can reliably follow the trend of barrier heights, which is very encouraging for researchers employing DFT as a tool to explore the reactivity mechanism and trends. Additionally, the slopes of the correlation lines of B3LYP, B2GP-PLYP, PBE0, and M06-L are very close to ideal 1.0 (deviation within 0.03 from 1.0), which is in line with their good performances in reproducing absolute barriers and which suggests that the barrier underestimation by these methods for these studied systems is small. The correlation here is much better than the ones found in our previous Au-, Ir-, and Pt-catalyzed reactions (with a best  $R^2$  to be around 0.9),<sup>18</sup> which cover five reaction types rather than the single one, as studied here. This observed difference in the quality of the correlations is reasonable, and it serves to underscore the message that comparisons of absolute DFT barrier values for different types of reactions may not be meaningful.

Finally, the empirical dispersion corrections, developed for DFT, were also tested in barrier height calculations. As before,<sup>18</sup> here too the dispersion effect shown in Table 2 is minor in these late-TM catalyzed reactions.

In this study, using the recently proposed corrective LCCSD(T0) method as a reference, we systematically assessed

the performance of tens of widely used DFTs in C–H bond activation barrier computations of late platinum group TM (Rh, Pd, Ir, Pt) pincer complexes. The pincer ligands explored cover a wide range of PNP, PCP, POCOP, NCN, and SCS types. Surprisingly, the B3LYP functional is found to be the most accurate one, followed by several other functionals like B2GP-PLYP, B2-PLYP, and PBE0, which were also found to perform well in many previous DFT calibration studies in TM systems.<sup>10,18,44</sup> Some interesting uniform trends for the accuracy of almost all DFT methods tested herein were observed: (1) group 9 TM (Rh and Ir) pincer complexes have higher accuracy than corresponding group 10 TM (Pd and Pt) ones of the same period; (2) within the same group, 5d TM pincer complexes have a higher accuracy than 4d TM ones. As a result, C–H activation energies of Pd pincer complexes were found to be the most difficult cases among the four TMs to almost all DFTs tested here. The DFT empirical dispersion correction (DFT-D3) is shown to have a very small effect on barrier height. Although this study includes only the C–H activation process, it is apparent that the results reported here have also some implications for other  $\sigma$ -bond activations like H–H, C–C, and C–halogen bonds by late platinum group pincer complexes.

## ■ ASSOCIATED CONTENT

### Supporting Information

Cartesian coordinates and six tables of computational results. This material is available free of charge via the Internet at <http://pubs.acs.org>.

## ■ AUTHOR INFORMATION

### Corresponding Author

\*E-mail: wenzhenlai@ruc.edu.cn (W.L.); chenh@iccas.ac.cn (H.C.).



## Notes

The authors declare no competing financial interest.

## ACKNOWLEDGMENTS

This work was supported by the Fundamental Research Funds for the Central Universities, the Research Funds of Renmin University of China (No. 12XNLJ04 to W.L.), and the Chinese Academy of Sciences (to H.C.). S.S. is supported by a special Minerva fund.

## REFERENCES

- (1) *The Chemistry of Pincer Compounds*; Morales-Morales, D.; Jensen, C. M., Eds.; Elsevier Science: Amsterdam, 2007.
- (2) Albrecht, M.; van Koten, G. *Angew. Chem., Int. Ed.* **2001**, *40*, 3750–3781.
- (3) (a) van der Boom, M. E.; Milstein, D. *Chem. Rev.* **2003**, *103*, 1759–1792. (b) Choi, J.; MacArthur, A. H. R.; Brookhart, M.; Goldman, A. S. *Chem. Rev.* **2011**, *111*, 1761–1779. (c) Selander, N.; Szabó, K. J. *Chem. Rev.* **2011**, *111*, 2048–2076.
- (4) (a) Benito-Garagorri, D.; Kirchner, K. *Acc. Chem. Rev.* **2008**, *41*, 201–213. (b) Haibach, M. C.; Kundu, S.; Brookhart, M.; Goldman, A. S. *Acc. Chem. Rev.* **2012**, *45*, 947–958. (c) Gunanathan, C.; Milstein, D. *Acc. Chem. Rev.* **2011**, *44*, 588–602. (d) Leis, W.; Mayer, H. A.; Kaska, W. C. *Coord. Chem. Rev.* **2008**, *252*, 1787–1797.
- (5) (a) Krogh-Jespersen, K.; Czerw, M.; Summa, N.; Renkema, K. B.; Achord, P. D.; Goldman, A. S. *J. Am. Chem. Soc.* **2002**, *124*, 11404–11416. (b) Krogh-Jespersen, K.; Czerw, M.; Zhu, K. M.; Singh, B.; Kanzelberger, M.; Darji, N.; Achord, P. D.; Renkema, K. B.; Goldman, A. S. *J. Am. Chem. Soc.* **2002**, *124*, 10797–10809. (c) Zhu, K. M.; Achord, P. D.; Zhang, X. W.; Krogh-Jespersen, K.; Goldman, A. S. *J. Am. Chem. Soc.* **2004**, *126*, 13044–13053. (d) Ghosh, R.; Zhang, X. W.; Achord, P. D.; Emge, T. J.; Krogh-Jespersen, K.; Goldman, A. S. *J. Am. Chem. Soc.* **2007**, *129*, 853–866. (e) Feller, M.; Karton, A.; Leitun, G.; Martin, J. M. L.; Milstein, D. *J. Am. Chem. Soc.* **2006**, *128*, 12400–12401. (f) Li, S. H.; Hall, M. B. *Organometallics* **2001**, *20*, 2153–2160. (g) Blug, M.; Heuclin, H.; Cantat, T.; Le Goff, X.-F.; Mézailles, N.; Le Floch, P. *Organometallics* **2009**, *28*, 1969–1972. (h) Zeng, G. X.; Guo, Y.; Li, S. H. *Inorg. Chem.* **2009**, *48*, 10257–10263. (i) Niu, S.; Hall, M. B. *J. Am. Chem. Soc.* **1999**, *121*, 3992–3999. (j) Kozuch, S.; Clarite, A. *ChemCatChem* **2011**, *3*, 1348–1353. (k) Mohammad, H. A. Y.; Grimm, J. C.; Eichele, K.; Mack, H.-G.; Speiser, B.; Novak, F.; Quintanilla, M. G.; Kaska, W. C.; Mayer, H. A. *Organometallics* **2002**, *21*, 5775–5784. (l) Yang, X. Z. *ACS Catal.* **2011**, *1*, 849–854. (m) Feng, Y. F.; Wang, C. S.; Fan, H. J. *J. Organomet. Chem.* **2011**, *696*, 4064–4069. (n) Doux, M.; Ricard, L.; Le Floch, P.; Jean, Y. *Organometallics* **2006**, *25*, 1101–1111. (o) Walter, M. D.; White, P. S.; Schauer, C. K.; Brookhart, M. *New J. Chem.* **2011**, *35*, 2884–2893. (p) Ess, D. H.; Goddard, W. A., III; Periana, R. A. *Organometallics* **2010**, *29*, 6459–6472. (q) Surawatanawong, P.; Ozerov, O. V. *Organometallics* **2011**, *30*, 2972–2979. (r) Cao, Z. X.; Hall, M. B. *Organometallics* **2000**, *19*, 3338–3346. (s) Sundermann, A.; Uzan, O.; Milstein, D.; Martin, J. M. L. *J. Am. Chem. Soc.* **2000**, *122*, 7095–7104. (t) Ostapowicz, T. G.; Hölscher, M.; Leitner, W. *Chem.—Eur. J.* **2011**, *17*, 10329–10338. (u) Young, K. J. H.; Meier, S. K.; Gonzales, J. M.; Oxgaard, J.; Goddard, W. A., III; Periana, R. A. *Organometallics* **2006**, *25*, 4734–4737. (v) Nowroozi-Isfahani, T.; Musaev, D. G.; Morokuma, K.; Gagné, M. R. *Organometallics* **2007**, *26*, 2540–2549. (w) Rajeev, R.; Sunoj, R. B. *Dalton Trans.* **2012**, *41*, 8430–8440. (x) Solin, N.; Kjellgren, J.; Szabó, K. J. *J. Am. Chem. Soc.* **2004**, *126*, 7026–7033. (y) Fulmer, G. R.; Muller, R. P.; Kemp, R. A.; Goldberg, K. I. *J. Am. Chem. Soc.* **2009**, *131*, 1346–1347. (z) Johnson, M. T.; Johansson, R.; Kondrashov, M. V.; Steyl, G.; Ahlquist, M. S. G.; Roodt, A.; Wendt, O. F. *Organometallics* **2010**, *29*, 3521–3529.
- (6) (a) Niu, S.; Hall, M. B. *Chem. Rev.* **2000**, *100*, 353–405. (b) Siegbahn, P. E. M.; Blomberg, M. R. A. *Chem. Rev.* **2000**, *100*, 421–437. (c) Torrent, M.; Solà, M.; Frenking, G. *Chem. Rev.* **2000**, *100*, 439–493. (d) Dedieu, A. *Chem. Rev.* **2000**, *100*, 543–600. (e) Noodleman, L.; Lovell, T.; Han, W.-G.; Li, J.; Himo, F. *Chem. Rev.* **2004**, *104*, 459–508. (f) Rotzinger, F. P. *Chem. Rev.* **2005**, *105*, 2003–2037. (g) Balcells, D.; Clot, E.; Eisenstein, O. *Chem. Rev.* **2010**, *110*, 749–823. (h) Shaik, S.; Cohen, S.; Wang, Y.; Chen, H.; Kumar, D.; Thiel, W. *Chem. Rev.* **2010**, *110*, 949–1017. (i) Ackermann, L. *Chem. Rev.* **2011**, *111*, 1315–1345. (j) Ziegler, T.; Autschbach, J. *Chem. Rev.* **2005**, *105*, 2695–2722.
- (7) de Jong, G. T.; Bickelhaupt, F. M. *J. Chem. Theory Comput.* **2006**, *2*, 322–335.
- (8) de Jong, G. T.; Geerke, D. P.; Diefenbach, A.; Solà, M.; Bickelhaupt, F. M. *J. Comput. Chem.* **2005**, *26*, 1006–1020.
- (9) de Jong, G. T.; Geerke, D. P.; Diefenbach, A.; Bickelhaupt, F. M. *Chem. Phys.* **2005**, *313*, 261–270.
- (10) Quintal, M. M.; Karton, A.; Iron, M. A.; Boese, A. D.; Martin, J. M. L. *J. Phys. Chem. A* **2006**, *110*, 709–716.
- (11) Piacenza, M.; Hyla-Kryspin, I.; Grimme, S. *J. Comput. Chem.* **2007**, *28*, 2275–2285.
- (12) Zhao, Y.; Truhlar, D. G. *J. Chem. Theory Comput.* **2009**, *5*, 324–333.
- (13) Anoop, A.; Thiel, W.; Neese, F. *J. Chem. Theory Comput.* **2010**, *6*, 3137–3144.
- (14) Chen, H.; Lai, W. Z.; Shaik, S. *J. Phys. Chem. Lett.* **2010**, *1*, 1533–1540.
- (15) Sun, X. L.; Huang, X. R.; Li, J. L.; Huo, R. P.; Sun, C. C. *J. Phys. Chem. A* **2012**, *116*, 1475–1485.
- (16) Li, H. X.; Lu, G.; Jiang, J. L.; Huang, F.; Wang, Z. X. *Organometallics* **2011**, *30*, 2349–2363.
- (17) Faza, O. N.; Rodríguez, R. Á.; López, C. S. *Theor. Chem. Acc.* **2011**, *128*, 647–661.
- (18) Kang, R. H.; Lai, W. Z.; Yao, J. N.; Shaik, S.; Chen, H. *J. Chem. Theory Comput.* **2012**, *8*, DOI: 10.1021/ct3003942.
- (19) (a) Perdew, J. P.; Burke, K.; Ernzerhof, M. *Phys. Rev. Lett.* **1996**, *77*, 3865–3868; Erratum. *Phys. Rev. Lett.* **1997**, *78*, 1396–1396. (b) Ernzerhof, M.; Scuseria, G. E. *J. Chem. Phys.* **1999**, *110*, 5029–5036. (c) Adamo, C.; Barone, V. *J. Chem. Phys.* **1999**, *110*, 6158–6170.
- (20) (a) Zhao, Y.; Truhlar, D. G. *J. Chem. Phys.* **2006**, *125*, 194101. (b) Zhao, Y.; Truhlar, D. G. *Theor. Chem. Acc.* **2008**, *120*, 215–241.
- (21) Tao, J.; Perdew, J. P.; Staroverov, V. N.; Scuseria, G. E. *Phys. Rev. Lett.* **2003**, *91*, 146401.
- (22) (a) Becke, A. D. *Phys. Rev. A* **1988**, *38*, 3098–3100. (b) Lee, C.; Yang, W.; Parr, R. G. *Phys. Rev. B* **1988**, *37*, 785–789. (c) Becke, A. D. *J. Chem. Phys.* **1993**, *98*, 5648–5652.
- (23) Karton, A.; Tarnopolsky, A.; Lamere, J.-F.; Schatz, G. C.; Martin, J. M. L. *J. Phys. Chem. A* **2008**, *112*, 12868–12886.
- (24) Grimme, S. *J. Chem. Phys.* **2006**, *124*, 034108.
- (25) Chai, J.-D.; Head-Gordon, M. *J. Chem. Phys.* **2008**, *128*, 084106.
- (26) Boese, A. D.; Martin, J. M. L. *J. Chem. Phys.* **2004**, *121*, 3405–3416.
- (27) (a) Schäfer, A.; Huber, C.; Ahlrichs, R. *J. Chem. Phys.* **1994**, *100*, 5829. (b) Eichkorn, K.; Weigend, F.; Treutler, O.; Ahlrichs, R. *Theor. Chem. Acc.* **1997**, *97*, 119–124.
- (28) (a) Peterson, K. A.; Figgen, D.; Dolg, M.; Stoll, H. *J. Chem. Phys.* **2007**, *126*, 124101. (b) Figgen, D.; Peterson, K. A.; Dolg, M.; Stoll, H. *J. Chem. Phys.* **2009**, *130*, 164108. (c) Dunning, T. H. *J. Chem. Phys.* **1989**, *90*, 1007–1023. (d) Dunning, T. H. J.; Peterson, K. A.; Wilson, A. K. *J. Chem. Phys.* **2001**, *114*, 9244–9253.
- (29) Andrae, D.; Häußermann, U.; Dolg, M.; Stoll, H.; Preuß, H. *Theor. Chim. Acta* **1990**, *77*, 123–141.
- (30) Frisch, M. J.; Trucks, G. W.; Schlegel, H. B.; Scuseria, G. E.; Robb, M. A.; Cheeseman, J. R.; Scalmani, G.; Barone, V.; Mennucci, B.; Petersson, G. A.; Nakatsuji, H.; Caricato, M.; Li, X.; Hratchian, H. P.; Izmaylov, A. F.; Bloino, J.; Zheng, G.; Sonnenberg, J. L.; Hada, M.; Ehara, M.; Toyota, K.; Fukuda, R.; Hasegawa, J.; Ishida, M.; Nakajima, T.; Honda, Y.; Kitao, O.; Nakai, H.; Vreven, T.; Montgomery, J. A., Jr.; Peralta, J. E.; Ogliaro, F.; Bearpark, M.; Heyd, J. J.; Brothers, E.; Kudin, K. N.; Staroverov, V. N.; Kobayashi, R.; Normand, J.; Raghavachari, K.; Rendell, A.; Burant, J. C.; Iyengar, S. S.; Tomasi, J.; Cossi, M.; Rega, N.; Millam, J. M.; Klene, M.; Knox, J. E.; Cross, J. B.; Bakken, V.; Adamo, C.; Jaramillo, J.; Gomperts, R.; Stratmann, R. E.; Yazyev, O.; Austin, A. J.; Cammi, R.; Pomelli, C.; Ochterski, J. W.; Martin, R. L.; Morokuma,

K.; Zakrzewski, V. G.; Voth, G. A.; Salvador, P.; Dannenberg, J. J.; Dapprich, S.; Daniels, A. D.; Farkas, O.; Foresman, J. B.; Ortiz, J. V.; Cioslowski, J.; Fox, D. J. *Gaussian 09*, revision C.01; Gaussian, Inc.: Wallingford, CT, 2009.

(31) Werner, H.-J.; Knowles, P. J.; Lindh, R.; Manby, F. R.; Schütz, M.; Celani, P.; Korona, T.; Mitrushenkov, A.; Rauhut, G.; Adler, T. B.; Amos, R. D.; Bernhardsson, A.; Berning, A.; Cooper, D. L.; Deegan, M. J. O.; Dobbyn, A. J.; Eckert, F.; Goll, E.; Hampel, C.; Hetzer, G.; Hrenar, T.; Knizia, G.; Köppl, C.; Liu, Y.; Lloyd, A. W.; Mata, R. A.; May, A. J.; McNicholas, S. J.; Meyer, W.; Mura, M. E.; Nicklass, A.; Palmieri, P.; Pflüger, K.; Pitzer, R.; Reiher, M.; Schumann, U.; Stoll, H.; Stone, A. J.; Tarroni, R.; Thorsteinsson, T.; Wang, M.; Wolf, A. MOLPRO, version 2010.1, a package of ab initio programs. See <http://www.molpro.net>.

(32) (a) Weigend, F.; Köhn, A.; Hättig, C. *J. Chem. Phys.* **2002**, *116*, 3175–3183. (b) Hill, J. G. *J. Chem. Phys.* **2011**, *135*, 044105. (c) Hill, J. G.; Platts, J. A. *J. Chem. Theory Comput.* **2009**, *5*, 500–505.

(33) (a) Zhong, S. J.; Barnes, E. C.; Petersson, G. A. *J. Chem. Phys.* **2008**, *129*, 184116. (b) Karton, A.; Martin, J. M. L. *Theor. Chem. Acc.* **2006**, *115*, 330–333.

(34) Truhlar, D. G. *Chem. Phys. Lett.* **1998**, *294*, 45–48.

(35) Neese, F.; Valeev, E. F. *J. Chem. Theory Comput.* **2011**, *7*, 33–43.

(36) Boughton, J. W.; Pulay, P. *J. Comput. Chem.* **1993**, *14*, 736–740.

(37) Chen, K. J.; Zhang, G. L.; Chen, H.; Yao, J. N.; Danovich, D.; Shaik, S. J. *J. Chem. Theory Comput.* **2012**, *8*, 1641–1645.

(38) Even with M06-L, for which Pd pincer complexes did not generate the largest MUD, Pd pincer complexes have the largest MaxD among all four TMs.

(39) Chai, J.-D.; Head-Gordon, M. *Phys. Chem. Chem. Phys.* **2008**, *10*, 6615–6620.

(40) Cramer, C. J.; Truhlar, D. G. *Phys. Chem. Chem. Phys.* **2009**, *11*, 10757–10816.

(41) Sousa, S. F.; Fernandes, P. A.; Ramos, M. J. *J. Phys. Chem. A* **2007**, *111*, 10439–10452.

(42) For B3LYP found to be best in DFT assessment studies, see: (a) Phung, Q. M.; Vancoillie, S.; Pierloot, K. A. *J. Chem. Theory Comput.* **2012**, *8*, 883–892. (b) Li, S. G.; Dixon, D. A. *J. Phys. Chem. A* **2007**, *111*, 11908–11921. (c) Ghosh, A.; Gonzalez, E.; Tangen, E.; Roos, B. O. *J. Phys. Chem. A* **2008**, *112*, 12792–12798. (d) Mayhall, N. J.; Raghavachari, K. *J. Phys. Chem. A* **2009**, *113*, 5170–5175.

(43) According to the number of occurrences of various functional names in journal titles and abstracts of published papers in 2011, analyzed from the ISI Web of Science (2012), B3LYP still dominates the DFT applications in chemistry with more than 50% of the references.

(44) Kang, R. H.; Chen, H.; Shaik, S.; Yao, J. N. *J. Chem. Theory Comput.* **2011**, *7*, 4002–4011.